Landscape and Urban Planning 165 (2017) 162–171

Contents lists available at ScienceDirect

Landscape and Urban Planning

journal homepage: www.elsevier.com/locate/landurbplan

Research Paper

Optimizing green space locations to reduce daytime and nighttime urban heat island effects in Phoenix, Arizona

Yujia Zhang[a,*], Alan T. Murray[b], B.L. Turner II[c]

[a] School of Geographical Sciences and Urban Planning, Arizona State University, Coor Hall, 5th Floor, 975 S. Myrtle Ave., Tempe, AZ 85287, United States
[b] Department of Geography, University of California at Santa Barbara, Santa Barbara, CA 93106, United States
[c] School of Geographical Sciences and Urban Planning, and School of Sustainability, Arizona State University, Tempe, AZ 85287, United States

ARTICLE INFO

Keywords:
Urban heat island
Green space cooling
Location optimization
Environmental services trade-offs
Climate change mitigation

ABSTRACT

The urban heat island effect is especially significant in semi-arid climates, generating a myriad of problems for large urban areas. Green space can mitigate warming, providing cooling benefits important to reducing energy consumption and improving human health. The arrangement of green space to reap the full potential of cooling benefits is a challenge, especially considering the diurnal variations of urban heat island effects. Surprisingly, methods that support the strategic placement of green space in the context of urban heat island are lacking. Integrating geographic information systems, remote sensing, spatial statistics and spatial optimization, we developed a framework to identify the best locations and configuration of new green space with respect to cooling benefits. The developed multi-objective model is applied to evaluate the diurnal cooling trade-offs in Phoenix, Arizona. As a result of optimal green space placement, significant cooling potentials can be achieved. A reduction of land surface temperature of approximately 1–2 °C locally and 0.5 °C regionally can be achieved by the addition of new green space. 96% of potential day and night cooling benefits can be achieved through simultaneous consideration. The results also demonstrate that clustered green space enhances local cooling because of the agglomeration effect; whereas, dispersed patterns lead to greater overall regional cooling. The optimization based framework can effectively inform planning decisions with regard to green space allocation to best ameliorate excessive heat.

1. Introduction

As cities grow, changes in urban land cover and geometry/morphology/architecture coupled with intensifying human activities have led to a modified thermal climate, particularly at night, forming an urban heat island (UHI) (Fan & Sailor, 2005; Voogt & Oke, 2003). This effect has significant implications for sustainability, with consequences for energy and water consumption, emissions of air pollutants and greenhouse gases, human health, and the emergence of regional heat islands (Arnfield, 2003; Georgescu et al., 2014; Hondula et al., 2012, 2014; Huang, Zhou, & Cadenasso, 2011; Sailor, 2001). The UHI effect is intense in Phoenix, Arizona, amplified by rapid and extensive urbanization with resulting temperature increases approximating 0.5 °C per decade (Grimm et al., 2008). Summers in Phoenix are characterized by peaks in energy use and increased residential water consumption as well as the emergence of extreme UHI "riskscapes" (Harlan, Brazel, Prashad, Stefanov, & Larsen, 2006; Jenerette, Harlan, Stefanov, & Martin, 2011; Ruddell, Harlan, Grossman-Clarke, & Buyantuyev, 2010; Wentz, Rode, Li, Tellman, & Turner, 2016).

Green space, an area partially or completely covered by grass, trees, shrubs, and/or other vegetation in the form of parks, golf courses, large gardens, and yards, can effectively reduce temperature through shading and evapotranspiration (Balling & Lolk, 1991; Chang, Li, & Chang, 2007; Spronken-Smith & Oke, 1998). Recognizing the potential to mitigate UHI, the City of Phoenix has launched a master plan that aims to increase the amount of green space (City of Phoenix, 2010). Consequently, an important question is where to site new green space in order to best realize potential cooling benefits. Improvements in measuring and modeling cooling benefits of green spaces are required, however, to make informed decisions.

On the measurement side, air temperature based studies have found that green space can be 1–3 °C, and sometimes even 5–7 °C, cooler than surrounding built-up areas (Chow, Pope, Martin, & Brazel, 2011; Spronken-Smith & Oke, 1998; Upmanis, Eliasson, & Lindqvist, 1998), with cooling impacts extending as much as several hundred meters beyond green space boundaries (Bowler, Buyung-Ali, Knight, & Pullin, 2010; Eliasson & Upmanis, 2000; Spronken-Smith, Oke, & Lowry,

* Corresponding author.
E-mail addresses: yzhan169@asu.edu (Y. Zhang), amurray@ucsb.edu (A.T. Murray), Billie.L.Turner@asu.edu (B.L. Turner).

http://dx.doi.org/10.1016/j.landurbplan.2017.04.009
Received 26 July 2016; Received in revised form 26 March 2017; Accepted 12 April 2017
Available online 31 May 2017
0169-2046/

2000). Air temperature measurements are not suitable for citywide studies, however, due to their small sample size and limited spatial coverage (Bowler et al., 2010). Derived from remotely sensed thermal infrared imagery, land surface temperature (LST) measures surface UHI (SUHI). LST shows significant correlation with air temperature and provides complete spatial coverage across an entire cityscape (Fung, Lam, Nichol, & Wong, 2009; Klok, Zwart, Verhagen, & Mauri, 2012; Nichol, Fung, Lam, & Wong, 2009). Extensive research has explored relationships between SUHI and urban land cover, especially with regard to vegetation (Buyantuyev & Wu, 2010; Li, Li, Middel, Harlan, & Brazel, 2016; Myint, Wentz, Brazel, & Quattrochi, 2013; Ren et al., 2013; Weng 2009; Zhou, Huang, & Cadenasso, 2011). Studies have suggested that land cover composition and configuration of the green space are strong predictors of its cooling effect (Cao, Onishi, Chen, & Imura, 2010; Li et al., 2013; Lin, Yu, Chang, Wu, & Zhang, 2015; Maimaitiyiming et al., 2014; Ren et al., 2013 Ren et al., 2013). Furthermore, local context and adjacent green space also have impacts on cooling (Cheng, Wei, Chen, Li, & Song, 2014; Lin et al., 2015; Spronken-Smith & Oke, 1998, 1999). Explicit linkages between cooling effects and the locations of green spaces are missing, however, causing difficulties for location model construction.

On the modeling side, micro-climate numerical models deal with surface energy balance, simulating thermodynamic processes for canopy layer UHI assessment (Chow et al., 2011; Erell, Pearlmutter, & Williamson, 2012; Fernández, Alvarez-Vázquez, García-Chan, Martínez, & Vázquez-Méndez, 2015; Middel, Chhetri, & Quay, 2015; Ng, Chen, Wang, & Yuan, 2012). Results from such models are rich in temporal scale but are limited in spatial extent, thus fail to capture intra-urban temperature variations. Combining broader scale spatial data, multi-objective optimization models have been applied recently to determine green space locations in the city, balancing various kinds of environmental benefits. Neema and Ohgai (2013) developed a multi-objective heuristic technique for optimizing the configuration of parks and open space with respect to air and water quality improvement as well as noise and temperature reduction. Zhang and Huang (2014) sought to minimize LST in the allocation of land uses within a multi-objective heuristic, where temperature is a regressed function of land use intensities. As yet, however, no current model has attempted to account for the agglomeration of cooling resulting from adjacent green spaces, which greatly affects their spatial allocation.

The above mentioned measuring and modeling gaps are addressed in this research using an integrated framework that combines remote sensing, GIS, spatial statistics and spatial optimization. Fine-scale remote sensing data can greatly improve model reality, allowing better representation of the intra-urban SUHI intensities. Incorporated with GIS, statistical and optimization models facilitate practical location decision making to enhance green space cooling. The study first quantifies and predicts direct and indirect cooling benefits of the green space using LST and land cover data, linking cooling effect with green space locations. The exact formulation and solution for green space allocation is developed next and explicitly accounts for agglomeration-based cooling. The multi-objective model developed here considers both daytime and nighttime cooling impacts, enabling trade-off solutions to be identified. The framework is applied to an area in central Phoenix.

2. Study area and data

The Phoenix metropolitan area, one of fastest growing urban regions in the U.S., is located on the northern edge of the Sonoran Desert. With a population approaching 1.5 million, the City of Phoenix comprises approximately 134,200 ha of land in the center of a much larger metropolitan area (Fig. 1). Dominated by a semi-arid climate, this region has mild winters and hot summers. The temperature in Phoenix commonly exceeds 38 °C on average for 110 days during the year, and reaches 43 °C or higher for 18 days. The average annual rainfall is about 210.82 mm. With rapid urbanization during the last 50 years, the mean daily air temperature has increased by 3.1 °C and the nighttime minimum temperature by 5 °C (Brazel, Selover, Vose, & Heisler, 2000). The city and metropolitan area confront major urban heat island effects and related water withdrawal problems, which are expected to be amplified by climate change over the coming years.

To address sustainability challenges, Phoenix adopted a master plan in 2010 that aimed to create a healthier and more livable city through strategic investment in more green space (City of Phoenix, 2010). Existing green space in the city varies in size, shape and vegetation cover, exhibiting different levels of cooling effects during the day and the night. As illustrated in Fig. 1, green space is distributed rather unevenly across the city. Low-income, ethnic minority neighborhoods tend to have less and smaller-sized green spaces, generally with sparse vegetation cover (Harlan et al., 2006). The aerial imagery in Fig. 1 shows the detailed study area, which is 8,800 ha in size. This area is low-income and has a mixture of low and high vegetation cover neighborhoods.

Associated data utilized in this study includes thermal temperature readings and a fine-scale land cover classification. The land surface temperature was derived from Advanced Spaceborne Thermal Emission and Reflection Radiometer (ASTER) data layers. The ASTER image consists of six bands for short-wave infrared, at 30 m resolution, and five bands of thermal infrared, at 90 m resolution (Yamaguchi et al., 1998). The ASTER_08 product was used for surface temperature extraction. In order to address the diurnal cooling effect variation, a consecutive night and day cloud-free image pair were selected (under clear and clam weather conditions) for a summer period: June 17, 2010 (22:00 at local time) and June 18, 2010 (11:00 at local time), respectively. Daytime and nighttime temperatures for these dates at 90 m resolution are shown in Fig. 2. The study area consists of 11,466 (126 by 91) pixels. The mean surface temperature of the area is 55.60 °C and 29.85 °C for day and night, respectively. According to the National Weather Service and the Arizona Meteorological network, five weather stations are located within the extent of the utilized ASTER image, and one is within the reported study area (Fig. 1). Table 1 shows the comparison between air temperature and corresponding LST values. This highlights significant daytime differences between the surface and air temperatures, because LST responds to direct solar radiation (Cao et al., 2010; Hartz, Prashad, Hedquist, Golden, & Brazel, 2006). During nighttime, the surface temperatures are slightly higher than air temperatures. Calm wind conditions enhance the positive association between LST and air temperature, whereas strong winds decouple the relationship (Stoll & Brazel, 1992).

Both daytime and nighttime effects are examined because of their combined impacts on human wellbeing, energy and water use, and environmental performance. The well-known consequences of extreme summer temperatures in the Phoenix area include human health (Harlan et al., 2006), increased demands on energy for cooling and water for landscaping (Wentz et al., 2016), and impacts on year-round tourism favored by the commercial sector (Gober et al., 2009). Perhaps less known are the nighttime UHI effects. These include extending energy use for cooling into evening, owing to daytime heat storage (Grimmond & Oke, 2002), and throughout the night, as well as providing a higher temperature base from which the daytime UHI effect builds (Stoll & Brazel, 1992). Interestingly, higher nighttime temperatures during the winter reduce the occurrence of frost and its dampening effect on insects and anthropods, which in turn increase pesticide use, among other impacts (Ruddell, Hoffman, Ahmad, & Brazel, 2013).

In addition, a 1 m land cover classification of metropolitan Phoenix was utilized. This data layer was created using aerial imagery from the National Agricultural Imagery Program. The 1 m aerial images have four bands (RGB and NIR) and were acquired for summer 2010. The images were classified using the object-based method, implemented using the eConigtion software (Li et al., 2014). The resulting land cover data layer included 12 land cover classes with an overall accuracy of

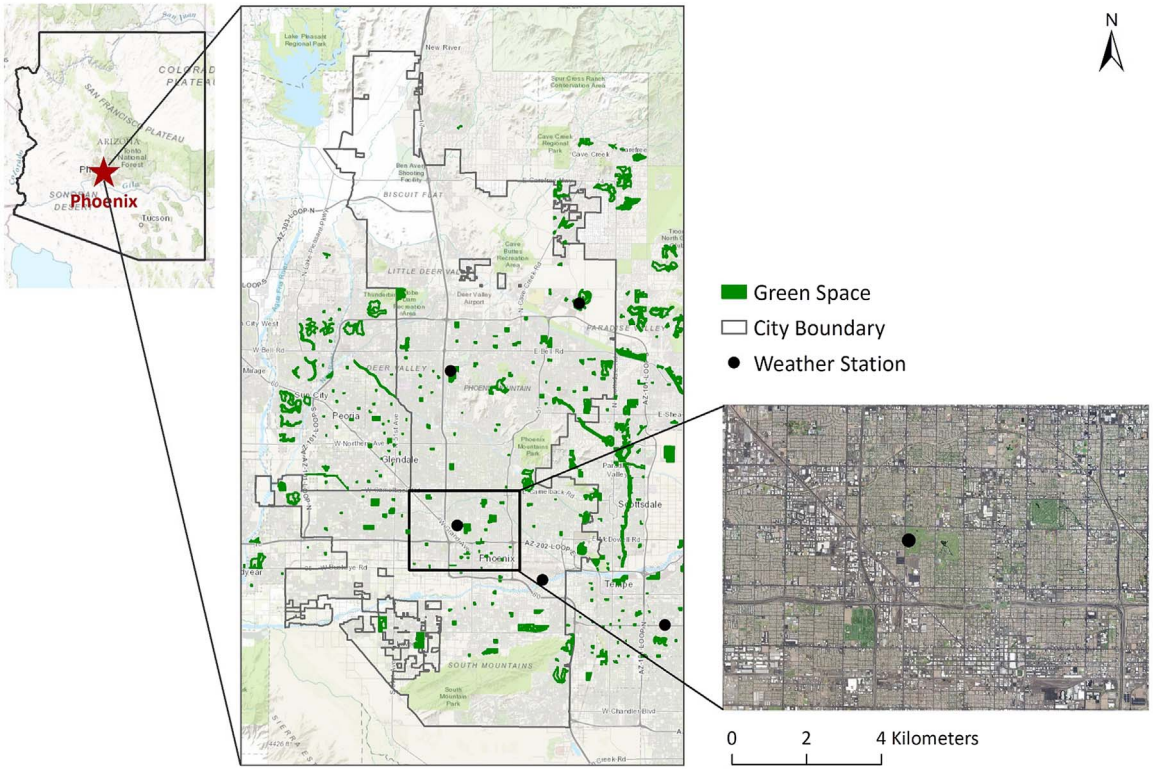

Fig. 1. City of Phoenix and study area.

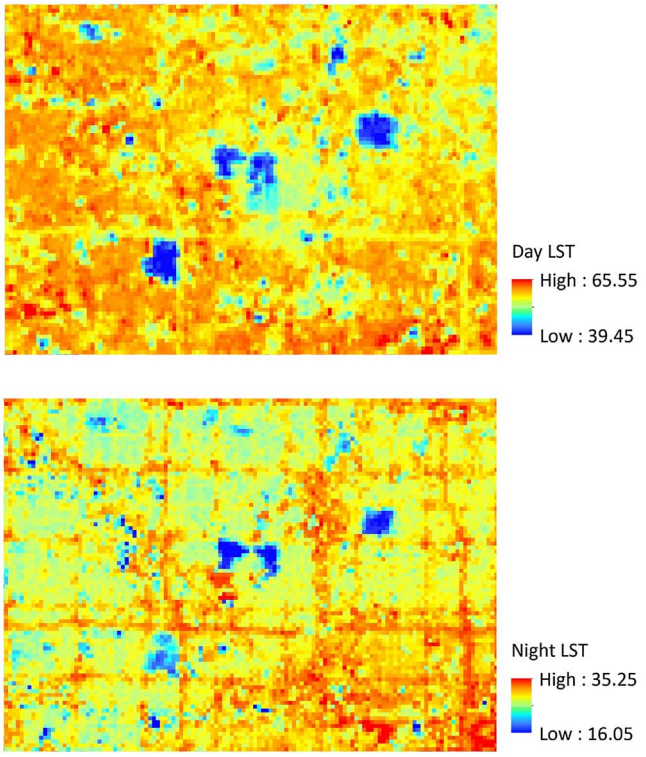

Fig. 2. Observed land surface temperature (LST) during the day and night (°C).

91.9%. For the purposes of this analysis, the 12 land cover classes were aggregated into 6 classes: building, paved surface, soil, tree (including shrub), grass and water (Fig. 3).

3. Methods

Fundamentally, green space provides local heat reduction that may contribute to region-wide benefits. Because of air movement and heat exchange, green space moderates temperatures within and beyond its boundaries, effectively forming neighborhood cooling (Ca, Asaeda, & Abu, 1998; Spronken-Smith & Oke, 1998; Spronken-Smith et al., 2000). Furthermore, the cooling effects of nearby green space may interact, enhancing local benefits (Lin et al., 2015; Spronken-Smith & Oke, 1999). A conceptualization of this is illustrated in Fig. 4. The thermal anisotropy of temperature is simplified, shown as a uniform distribution of the mean value for a given area. This not only indicates the direct benefits associated with green space, but also the indirect benefits to neighboring areas.

These basic types of cooling benefits (Fig. 4) can be characterized mathematically. For a given area i (or cell, parcel or land management zone), let β_i represent the temperature reduction possible if it is green space and δ_{ik} indicates the temperature reduction possible if there are k nearby green spaces. Given the temperature for an area as it currently exists, T_i, and the anticipated temperature if it were to be converted to green space, T_i^*, then the direct cooling benefit to area i is derived as follows:

$$\beta_i = T_i - T_i^* \quad (1)$$

Similarly, indirect cooling benefits can be derived as well:

$$\delta_{ik} = T_i - T_{ik}^{'} \quad (2)$$

where $T_{ik}^{'}$ denotes the anticipated temperature for area i if exactly k green spaces are neighboring i. Eqs. (1) and (2) therefore represent measures of potential benefit associate green space allocation and can be used in a land use planning process once they have been derived. In this case, T_i is estimated using the mean temperature of the local surrounding, which reflects the temperature without the cooling effect. Proximity corresponding to neighborhood and the local surrounding extent can be quantified, as is done here based on distance maximums.

Table 1
Comparison of air temperature and land surface temperature in °C.

Weather Station (from South to North)	Air Temperature (at 11:00)	Land Surface Temperature (at 11:00)	Air Temperature (at 22:00)	Land Surface Temperature (at 22:00)
Mesa	35.00	53.65	30.78	30.95
Phoenix Sky Harbor	35.33	56.75	33.61	31.35
Phoenix Encanto	**34.50**	**44.95**	**25.72**	**26.80**
Phoenix Greenway	34.00	45.85	27.78	27.35
Desert Ridge	32.39	45.35	25.61	28.15

The bold line indicates the weather station within the study area.

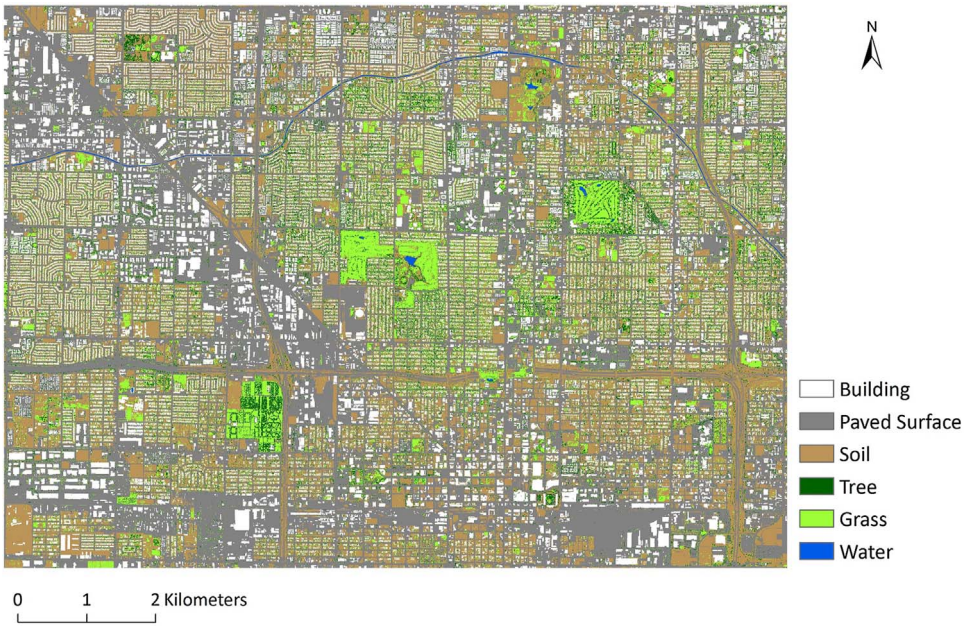

Fig. 3. Land cover data layer (1 m resolution).

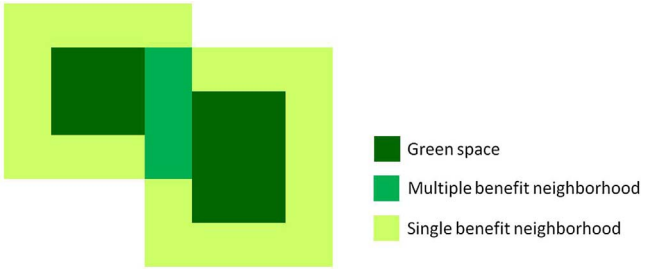

Fig. 4. Simplified distribution of green space cooling effects. (For interpretation of the references to color in this figure legend, the reader is referred to the web version of this article.)

To address urban heat island challenges, a spatial analytic framework that incorporates remote sensing, GIS, spatial statistics, and spatial optimization (Fig. 5) is proposed. Remote sensing provides essential data inputs, such as land cover and surface temperature measurements. GIS offers methods for integration and management of spatial information, important spatial analytic functions for deriving β_i and δ_{ik}, capability to structure the optimization model based on data inputs, and support to visualize and evaluate green space planning results. Spatial statistical analysis is used to predict cooling benefits, β_i and δ_{ik}, based on observed temperature, T_i, and land cover variables within and surrounding an area *i*. Spatial optimization is used for formalizing and solving the green space planning model. Each component requires data from or contributes data to GIS. Particularly important, however, are derived parameters and spatial information layers that are fed back into GIS.

3.1. Remote sensing

The thermal imagery supports green space optimization through the extraction of surface temperature across a region. This is far more comprehensive and complete than traditional spatial sampling approaches that rely on ground based equipment readings combined with interpolation. The surface temperature measurements were derived using ASTER_08 imagery, as noted previously. The data contains surface readings in Kelvin, corrected for atmospheric transmission, emissivity, absorption and path radiance (Gillespie, Rokugawa, Hook, Matsunaga, & Kahle, 1999). The absolute accuracy of the measures ranges from 1 to 4 K, with relative accuracy of 0.3 K (JPL, 2001). The readings were then converted to Celsius. The output is observed land surface temperature, T_i, for each of the 11,466 land units (cells) in the study area. The 1 m land cover data layer was classified using the object-based method based on the four bands aerial imagery, also noted previously. The aerial imagery was first segmented into parcel sized objects using cadastral parcel boundaries. Then, integrating spectral, contextual, geometrical information and expert knowledge, a hierarchical classification rule set was created to further assign and segment the image objects into detailed land cover classes (see Li et al., 2014). The result 1 m land cover map avoids the mixed feature problem of low-resolution data. Thus, it effectively depicts small, fragmented green space and enables examination of individual land cover effect on cooling (Li, Zhou, & Ouyang, 2013; Myint et al., 2013).The output is land cover, Z_i, for each of the 11,466 land units (cells) in the study area. ERDAS IMAGINE was utilized for all remote sensing processing.

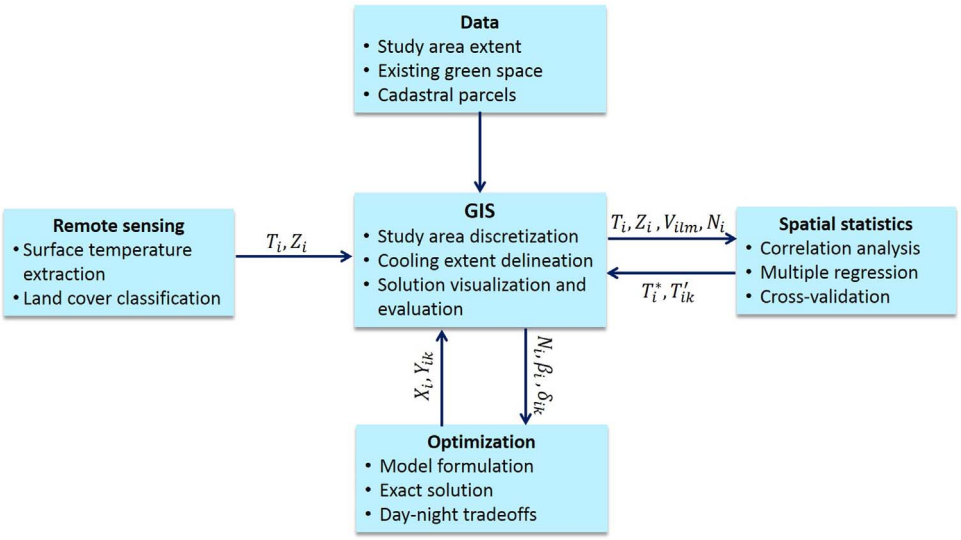

Fig. 5. Methodological framework.

3.2. GIS

GIS is a central component in this framework, connecting remote sensing, spatial statistical and optimization through data management, manipulation, analysis and visualization. The study area was first discretized into 11,466 land units (cells), with each cell of the size of 0.81 ha. Next, neighbor and local area buffers were delineated for each area i at 90 m and 360 m, respectively, based on observed temperature gradients around green space. Land cover variables, V_{ilm}, were derived using FRAGSTATS, a spatial analytical software for landscape analysis (McGarigal & Marks, 1995). The subscripts of V_{ilm} indicate variable type l (e.g., percent cover, shape index, mean patch area, etc.) by zone m (e.g., green space, neighborhood, local, etc.) for each area i. Another proximity based attribute derived using GIS was adjacency, where neighboring units are in the set N_i for each area i, which is associated with the indirect cooling. This information is utilized in land cover evaluation, statistical analysis and optimization. A final aspect of GIS is that results from statistical analysis and spatial optimization are readily displayed for evaluation in various ways. ArcGIS was utilized for all GIS processing.

3.3. Statistical analysis

As noted previously, research has established that size, shape and land cover of green space are strong predictors of its cooling effect. Furthermore, cooling benefit is location dependent, affected by the surrounding land cover as well (Cheng et al., 2015). The formal specification of cooling benefits are given in Eqs. (1) and (2). Critical of course is the estimated temperatures associated with green space, T_i^* and $T_{ik}^{'}$, where the former is expected temperature if area i is converted to green space and the latter is the expected temperature when exactly k green spaces are nearby. In general, expected temperature is a function of a variety of observed characteristics for each area (and/or neighboring areas):

$$T_i^* = f(T_i, Z_i, V_{ilm}, N_i) \tag{3}$$

$$T_{ik}^{'} = g(j \in N_i, Z_j, T_j, V_{jlm}) \tag{4}$$

Again, T_i^* and $T_{ik}^{'}$ are needed for deriving benefits, β_i and δ_{ik}, as detailed in Eqs. (1) and (2). Precise mathematical specification is based on components of the spatial statistical module of the framework involving correlation analysis, multiple linear regression, and cross-validation methods. Model fitness was statistically significant, with no issues of spatial autocorrelation or multi-collinearity. More than 300 observed green space areas in Phoenix enabled appropriate parameters to be derived for temperature estimation in both day and night conditions. SPSS and R package were utilized for all statistical analysis.

3.4. Optimization

An optimization model was structured to identify the best locations for new green space in order to realize the greatest overall benefits associated with day-night cooling trade-offs. The approach taken extends the coverage location model of Church and ReVelle (1974) (see also Church & Murray 2009; Murray, Tong, & Kim, 2010) in a number of ways. Specially, the nature of benefits differs, where β_i accounts for direct cooling benefits. In addition, there is a need to track indirect cooling benefits, where k explicitly notes the number of times an area neighbors green space. In the objective, δ_{ik} accounts for the indirect cooling enhancement associated with k. The notation of the discrete integer optimization model is defined as follows:

j = index of potential green space areas
i = index of areas
k = number of neighboring green spaces
β_j = direct cooling benefit for converting area j to green space
δ_{ik} = indirect cooling benefit area i received from k neighboring green spaces
N_i = set of areas neighboring unit i
p = number of green spaces to locate in a region

$$X_j = \begin{cases} 1 & \text{if area } j \text{ converted to green space} \\ 0 & \text{if not} \end{cases}$$

$$Y_{ik} = \begin{cases} 1 & \text{if area } i \text{ neighbors } k \text{ green spaces} \\ 0 & \text{if not} \end{cases}$$

The developed coverage is formulated as follows:

$$Maximize \sum_j \beta_j X_j + \sum_i \sum_k \delta_{ik} Y_{ik} \tag{5}$$

Subject to

$$kY_{ik} - \sum_{j \in N_i} X_j \leq 0 \quad \forall\, j, k \tag{6}$$

$$\sum_k Y_{ik} + X_i \leq 1 \quad \forall\, i \tag{7}$$

$$\sum_j X_j = p \tag{8}$$

$$X_j = \{0, 1\} \quad \forall\ j$$
$$Y_{ik} = \{0, 1\} \quad \forall\ i, k \tag{9}$$

The objective, (5), is to maximize the total sum of cooling benefits, either directly or indirectly. Constraints (6) define whether indirect cooling benefit is provided to area *i*. Constraints (7) ensure that at most one of the two types of cooling benefits is provided to an area. Constraint (8) specifies that *p* areas are to be converted to green space. The value of *p* is predetermined base on the goals associated with the city's plan. Finally, binary restrictions are imposed on decision variables in Constraints (9).

Of particular note within the context of the methodological framework, the primary output that would be fed back into GIS is the decision variable values, X_j and Y_{ik}. That is, which areas are selected for conversion to green space and which areas benefit from indirect cooling. Somewhat complicating things associated with this model is that it can be applied to daytime or nighttime conditions. Viewed in this way, trade-offs are possible when day and night are simultaneously considered. To do this, a weighted multi-objective model can be structured. Assume the following:

$$\Omega_{day} = \sum_j \beta_j X_j + \sum_i \sum_k \delta_{ik} Y_{ik} \tag{10}$$

$$\Omega_{night} = \sum_j \beta_j X_j + \sum_i \sum_k \delta_{ik} Y_{ik} \tag{11}$$

What changes between (10) and (11) are the values of β_j and δ_{ik} depending on whether it is day or night conditions. The two objectives can be integrated using a weighting variable *w* as follows:

$$Maximize \quad w\Omega_{day} + (1 - w)\Omega_{night} \tag{12}$$

where $w \in [0,1]$. Thus, this model can be repeatedly solved for different values of *w*, with each unique solution representing a valid and potentially meaningful trade-off solution. Planning and decision making processes would therefore take this information into account prior to plan implementation.

The analysis was carried out on an Intel i5 (3.10 GHz) computer running Windows 7 64-bit with 8 GB of RAM. ArcGIS 10.2 was used to discretize the study area and delineate the cooling coverage. Arcpy and Gurobi python API were employed to import the location information and constructed the mixed integer model. The model was then solved in Gurobi using the branch-and-bound approach. The original model contained 2,935,297 rows, 2,935,552 columns and 16,511,232 nonzero elements. The presolve process in Gurobi first tightens the formulation, with a reduced model size of 93,899 rows and 377,020 columns, with 1,120,292 nonzero elements. The linear relaxation is used to establish an upper bound, with feasible integer solutions establishing valid lower bounds. The optimality gap between the upper and lower bound converges to zero within three minutes through the use of branch and bound.

4. Results

4.1. Observed and predicted cooling benefits

Fig. 6 summarizes the observed cooling benefits based on green space samples in the Phoenix area. Computation of the direct and indirect cooling benefits are based on Eqs. (1) and (2). T_i was estimated using the mean temperature of the local buffers (360 m). The direct benefit, β_i, is obtained by computing the temperature differences between the green space and its local buffer. The mean observed direct benefit for the daytime is 4.17 °C and 2.33 °C for the nighttime.

Calculation of the indirect benefit δ_{ik} is more complicated, requiring separation of the neighboring area of green space (Fig. 4). The single and multiple coverage polygons are identified and extracted using spatial relationship operations in ArcGIS, such as intersect and merge.

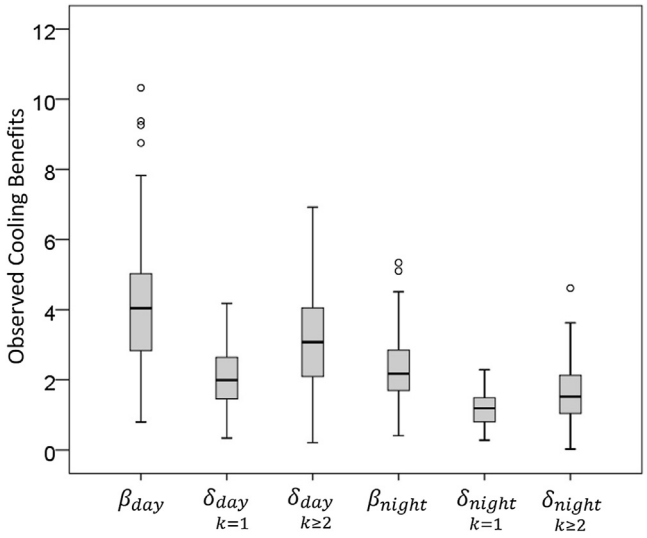

Fig. 6. Observed cooling benefits (in °C).

Fig. 6 demonstrates significant indirect cooling effects on neighboring area of green space. During the daytime, when $k = 1$, the observed mean value of indirect benefit (δ_{ik}) is 2.04 °C. However, when $k \geq 2$, the mean value of indirect benefit increases to 3.12 °C. During the nighttime, the observed mean value is 1.18 °C ($k = 1$) and increased to 1.61 °C for $k \geq 2$.

Fig. 7 summarizes the predicted β_i across the study area, which was the direct cooling benefit for area *i* if it is converted to green space. The daytime mean value is 6.7 °C. The nighttime mean value is 2.6 °C. We assume the green conversion had identical land cover, which is 100% grass. Grass cover is selected because of its simpler effects on radiation and surface energy balance compared to trees. Unlike grass, trees affect cooling in positive and negative ways. Shading and evapotranspiration

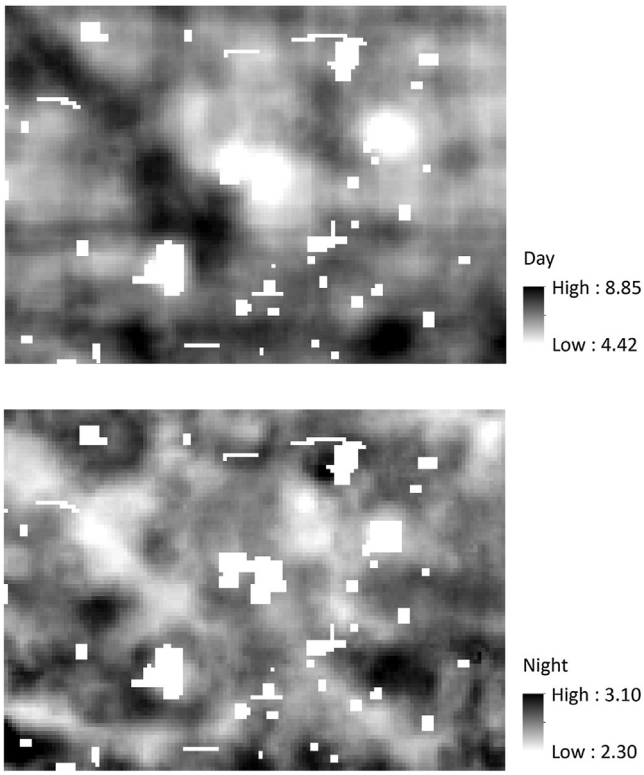

Fig. 7. Predicted direct cooling benefits (in °C, excluding existing green space and water bodies).

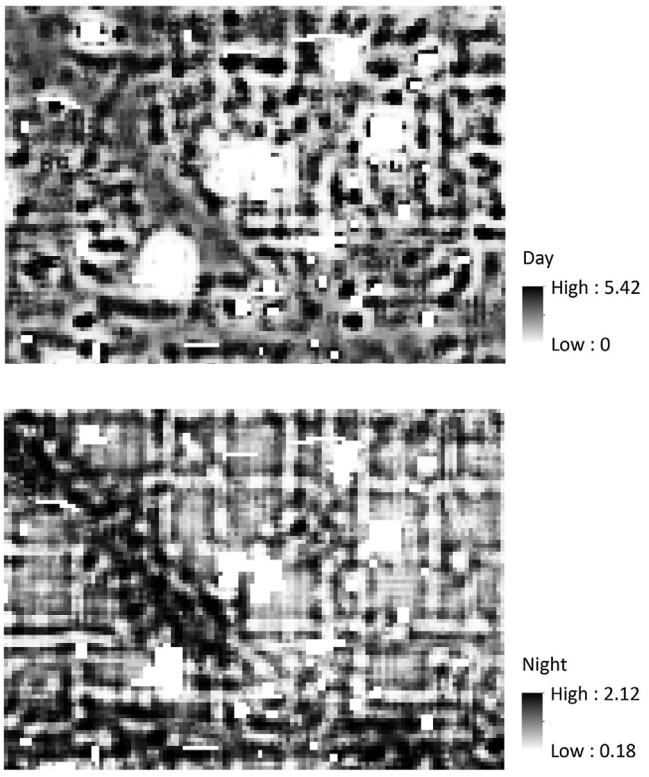

Fig. 8. Predicted indirect cooling benefits (k = 1 case, in ˚C, excluding existing green space and water bodies).

facilitate cooling. Trees also lower wind speed and reduce advection, however, which may decrease the cooling effect. In addition, during nighttime, tree canopies inhibit long-wave radiative cooling by blocking part of the skyview, while excess moisture increases the thermal capacity of the soil and slows down surface cooling (Erell et al., 2012).

When area i is converted to green space, it also distributes indirect cooling benefits to neighboring land, eight areas in this case. The predicted indirect cooling benefit estimations are summarized in Fig. 8 for the case of a single neighboring green space (k = 1, so δ_{i1}). The mean daytime and nighttime δ_{i1} are 2.7 ˚C and 1 ˚C, respectively. Spatially, Fig. 8 is much patchier compared to Fig. 7. The patchy pattern (steep values changes within short distance) highlights potential cooling centers in the study area. For example, during the daytime, the local cooling centers are places that have a high percent of vegetation cover or complex shaped buildings within their neighborhood, and low percent of vegetation cover beyond. At nighttime, however, local cooling centers change to places that have high contrast between the percent cover and shape of the paved surface within and beyond their neighborhood. While not shown here, multiple neighboring green spaces will enhance local cooling. This is reflected in the cases when $k \geq 2$ for δ_{ik}.

4.2. Day-night cooling trade-offs

The optimization model allows for any level of green space allocation to be evaluated, but the results presented here are necessarily focused on the city's plan objective. Consequently, in this analysis it is assumed that 150 land units will undergo conversion to green space, thus p = 150. This equates to 121.5 ha of new green space (1.3% of the study area). Table 2 summarizes the trade-off solutions identified when the importance weight for day and night cooling benefits is varied. When w = 1, daytime cooling benefits are considered to be the most important. The result, Ω_{day}, corresponds to 5,479.80 ˚C in total temperature reduction across all cells in the study area. Associated with this allocation of green space, the nighttime cooling benefit is 1908.02 ˚C in column 4. Alternatively, when w = 0, this represents the case where nighttime cooling benefits are deemed most important, and the objective value, Ω_{night}, is 2,233.94 ˚C. Associated with this pattern of green space would be a total daytime cooling benefit of 4738.28 ˚C. These two situations highlight that optimizing daytime benefit is not equivalent to optimizing nighttime benefit. As such, compromise green space selection solutions can be identified that consider both day and night cooling benefits simultaneously by varying the value of w, reported in Table 2.

Table 2
Trade-offs associated with day and night cooling benefits.

w	Ω_{day}	Day: % of obj. decreased	Ω_{night}	Night: % of obj. decreased
1	5479.80	0.00%	1908.02	14.59%
0.9	5479.27	0.01%	1917.52	14.16%
0.8	5476.91	0.05%	1931.42	13.54%
0.7	5466.80	0.24%	1959.69	12.28%
0.6	5442.68	0.68%	2002.95	10.34%
0.5	5401.44	1.43%	2053.49	8.08%
0.4	5328.01	2.77%	2110.58	5.52%
0.3	5256.25	4.08%	2148.13	3.84%
0.2	5111.26	6.73%	2194.82	1.75%
0.1	4957.13	9.54%	2221.46	0.56%
0	4738.28	13.53%	2233.94	0.00%

Fig. 9 depicts the trade-off solutions of the Ω_{day} and Ω_{night} columns in Table 2 for each value of w. Included in this figure are green space distributions of three trade-off solutions, where the w = 1 (importance on daytime cooling benefits) green space pattern is shown closest to the x-axis, the w = 0 (importance on nighttime cooling benefits) pattern is shown closest to the y-axis, and the w = 0.3 pattern is in between. The latter is a compromise between the two competing objectives. The patterns vary spatially, which is not surprising considering the variation reflected in predicted cooling benefits detailed in Figs. 7 and 8.

The optimal green space allocations lead to dramatic gains in local cooling benefits. Day conditions resulted in direct and indirect benefits of 6.68 ˚C and 3.74 ˚C on average, respectively, which is about 2 ˚C higher than means for observed, existing green space cooling benefits in the study area. Similarly, night condition local cooling benefits were able to be increase some 1 ˚C–2.57 ˚C and 1.55 ˚C (direct and indirect, respectively) on average. Beyond this, a significant drop in regional average temperature across the study area is also observed. The mean observed temperature in the study area is 55.60 ˚C and 29.85 ˚C for day and night, respectively (see Fig. 2). The greatest reduction in average temperature during the day is associated with the green space pattern when w = 1, reducing temperature to 55.13 ˚C. This represents almost 0.5 ˚C less than the current average in the study area of 55.60 ˚C. The greatest reduction in nighttime average temperature is the green space pattern when w = 0, reducing temperature to 29.66 ˚C (a 0.19 ˚C decrease from current average temperature). Trade-off solutions, therefore, range between these extremes. For the green space pattern when w = 0.3, average daytime temperature is 55.15 ˚C and the nighttime average temperature is 29.67 ˚C.

The spatial heterogeneity of cooling benefits associated with green space allocation solution is depicted in Fig. 10 for the case when w = 0 (importance on nighttime cooling). This illustrates not only where the green space is to be located, but also the derived direct and indirect cooling values. The selected locations are consistent with existing findings on nighttime SUHI, which suggest that areas of abundant impervious cover have higher impact on cooling than vegetated area at night (Buyantuyev & Wu, 2010; Myint et al., 2013). As demonstrated in Fig. 10, places along the industrial corridor and nearby the airport have the highest potential for nighttime cooling. In contrast, highly vegetated neighborhoods observe minimal new green space allocation. Of note is the agglomeration of indirect cooling benefit captured in this case (inset image shown in Fig. 10). The overlapped neighborhood

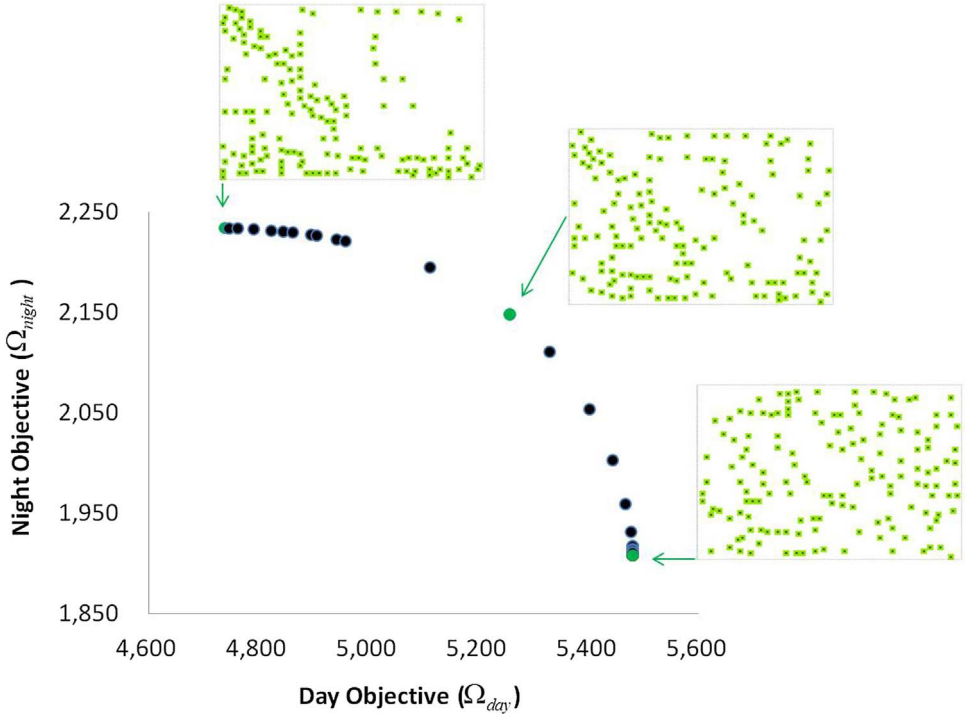

Fig. 9. Day-night trade-off solutions (in ˚C).

received 0.6 ˚C higher cooling than the single coverage neighborhood. It proves beneficial to ensure in this case that indirect local benefit is enhanced. That is, capturing the contribution of local benefits ($k \geq 2$) is favored. The model is able to strategically account for this in order to maximize regional cooling benefits

5. Discussion

It is well known that increasing green spaces in urban areas helps to ameliorate the extremes of UHI and SUHI effects. The research dedicated to this relationship has largely focused on the amount or area of green spaces, although increasing attention has focused on the broader characteristics of the pattern of green spaces such as concentration or dispersion (Myint et al., 2015). To our knowledge, however, no attempts have been made to determine the optimal locations for green spaces accounting for diurnal UHI variations, creating an information lacuna for decision makers confronting the negative impacts of excessive urban temperatures (e.g., Hondula, Vanos, & Gosling, 2014). Our framework effectively addresses this issue by integrating GIS, remote sensing and spatial statistics with optimization modeling. The model links green space allocation with local landscape context and enables identification of trade-off solutions that balance diurnal cooling benefits.

5.1. General implications of UHI reduction

The results suggest that optimal green space siting may lead to 1–2 ˚C local LST reduction and nearly 0.5 ˚C regional LST reduction, on average, throughout the Phoenix study area. This is remarkable given that the new green space was limited to only 1.3% of the study area.

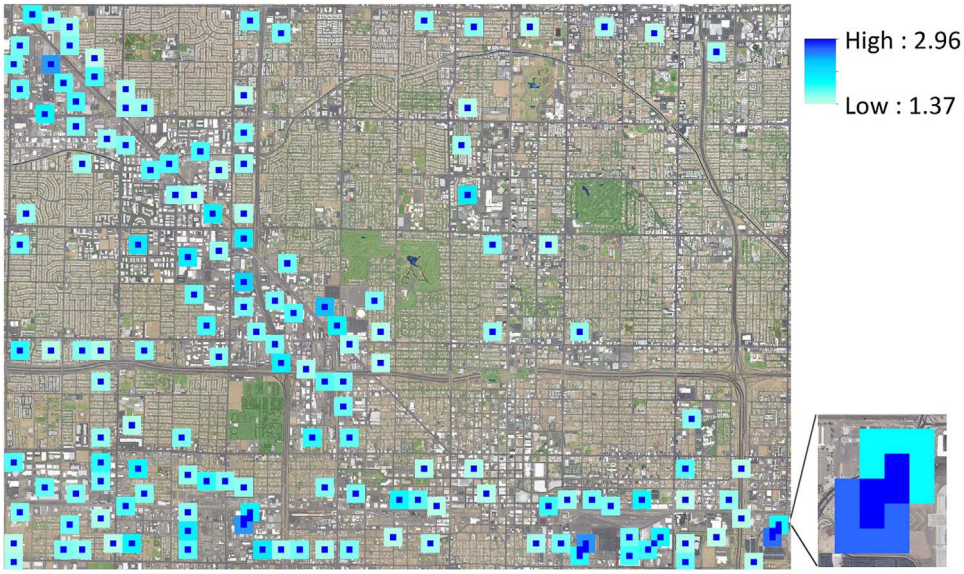

Fig. 10. Green space allocation pattern ($w = 0$). (For interpretation of the references to color in this figure legend, the reader is referred to the web version of this article.)

There may well be increased benefits if more green space is considered. Other research beyond Phoenix indicates that a similar reduction in air temperature, to which LST contributes, leads to a decrease of up to 10% in peak energy demand (Fung, Lam, Hung, Pang, & Lee, 2006; Meier & Taha, 2000). The consequences for water use are more complex, however. Green spaces, such as the turf grass assumed in this study, require substantial water in desert cities. All turf grass and non-native vegetation in Phoenix is irrigated, and outdoor water application currently accounts for a majority of residential and neighborhood water use in the metropolitan area (Balling, Gober, & Jones, 2008; Gober et al., 2009; Wentz et al., 2016). As a result, adding more green space may increase water demand, but the rate of use might be lowered by incorporating mixed vegetation. Research in the Negev Desert in Israel, for example, found that a combination of grass covered by shade trees or mesh shading created a synergy with greater cooling and led to a 50% reduction in water use (Shashua-Bar, Pearlmutter, & Erell, 2009). Finally, ameliorating temperature extremes is known to have positive health impacts (e.g., Hondula et al., 2012).

5.2. Trade-offs of green space cooling

Beyond temperature reduction, this study also provides valuable insights on green space patterning in relation to cooling trade-offs. Our finding is consistent with existing research that the concentration of green spaces enhances local cooling (Chang et al., 2007; Spronken-Smith & Oke, 1999). Such observations, however, do not consider the trade-offs between local and regional cooling benefits. Our model demonstrated that, although clustered pattern enhances local cooling, their overall regional cooling benefit is lower than the spatially dispersed pattern (see Fig. 9). This is because the dispersed pattern ultimately influences a larger area through the local cooling provided to adjacent parcels of land. In addition, other studies in the Phoenix area have observed the varied diurnal role of different land covers on SUHI (Buyantuyev & Wu, 2010; Myint et al., 2013). As of yet, however, minimal attention has been given to the evaluation of trade-offs between day and night relative to an established pattern of land cover (Turner, Janetos, Verburg, & Murray, 2013). Our modeling approach addresses this, indicating that maximized daytime cooling of green spaces results in an approximately 15% reduction in nighttime cooling and vice versa. Optimizing for both day and night simultaneously, it is possible to achieve some 96% of the potential cooling benefits.

5.3. Limitations and future research avenues

The model results are significant and point to the utility of such approaches. Our framework, however, is a first-generation effort and as such has a number of limitations that require attention in future research. For example, distance decay patterns of the cooling benefit were simplified to an “all or nothing” coverage assumption based on a fixed cooling extent. Future development could relax this assumption using a general coverage function representing the proportion of cooling benefit obtained at a certain distance from the green space (see Berman, Drezner, & Krass, 2010). In addition, an isotropic surface temperature distribution was employed, in which the temperature is represented by its mean value within a given area. In reality, the cooling effect varies spatially in different directions, which would potentially affect the extent and the interactions of cooling among adjacent green areas (see Lin et al., 2015). It is also worth noting that indirect cooling benefits could be more extensive than represented in the modeling framework. It is likely that our approach has underestimated the indirect cooling benefits, δ_{ik}, which may have implications on the spatial pattern of optimal green spaces. Further study requires more adjacent green space samples to better quantify indirect cooling. In this case, linear modeling is employed to better interpret variable effects. In general then, it is clear that estimation of direct and indirect benefits is an important area for future research, both in terms of the quality of estimates but also in terms of green space selection impact. For example, the non-linear relationship between cooling benefit and the size of green space has been reported in several studies (Cao et al., 2010; Chang et al., 2007). On the modeling side, parameter value changes and sensitivities could also be explored. As noted previously, more new green space could be considered, which would involve increasing the parameter p and re-running the optimization models. The relationship between green space allocation and regional temperature response certainly is an area for more research.

6. Conclusions

Our integrated framework demonstrates significant cooling potentials can be gained through optimal green space placement in Phoenix, Arizona. Daytime and nighttime cooling trade-offs are examined because of their combined impacts on human wellbeing, energy and water use, and environmental performance. In addition to size, land cover, and shape, green space optimization also depends on the surrounding land cover context, agglomeration of cooling resulting from adjacent green spaces and diurnal heat island variations. The selected optimal locations enhance landscape heterogeneity at the local scale, which would increase the surface temperature gradients and potentially accelerate air flow, preventing daytime heat storage and facilitating nighttime cooling. The developed model can be further applied to assess different land arrangements for various cooling considerations. Our findings help to address the growing environmental problem of extreme temperatures confronting urban areas worldwide.

Acknowledgements

This research was supported by the Central Arizona-Phoenix Long-Term Ecological Research program (NSF Grant No. BCS-1026865), the Decision Center for a Desert City (NSF Grant No. SES-0951366), National Science Foundation (NSF) under Grant No. SES-0951366, NSF DNS Grant No. 1419593 and USDA NIFA Grant No. 2015-67003-23508, the Julie Ann Wrigley Global Institute of Sustainability. The research was undertaken in the Environmental Remote Sensing and Geoinformatics Lab, Arizona State University. We thank for the valuable inputs from Dr. Anthony Brazel and our reviewers.

References

Arnfield, A. J. (2003). Two decades of urban climate research: A review of turbulence, exchanges of energy and water, and the urban heat island. *International Journal of Climatology*, *23*(1), 1–26.

Balling, R., & Lolk, N. (1991). A developing cool island in the desert? The case of Palm Springs, California. *Journal of the Arizona-Nevada Academy of Science*, *23*(2), 93–96.

Balling, R. C., Gober, P., & Jones, N. (2008). Sensitivity of residential water consumption to variations in climate: An intraurban analysis of Phoenix, Arizona. *Water Resources Research*, *44*(10).

Berman, O., Drezner, Z., & Krass, D. (2010). Generalized coverage: New developments in covering location models. *Computers & Operations Research*, *37*(10), 1675–1687.

Bowler, D. E., Buyung-Ali, L., Knight, T. M., & Pullin, A. S. (2010). Urban greening to cool towns and cities: A systematic review of the empirical evidence. *Landscape and Urban Planning*, *97*(3), 147–155.

Brazel, A., Selover, N., Vose, R., & Heisler, G. (2000). The tale of two climates Baltimore and Phoenix urban LTER sites. *Climate Research*, *15*(2), 123–135.

Buyantuyev, A., & Wu, J. (2010). Urban heat islands and landscape heterogeneity: Linking spatiotemporal variations in surface temperatures to land-cover and socioeconomic patterns. *Landscape Ecology*, *25*(1), 17–33.

Ca, V. T., Asaeda, T., & Abu, E. M. (1998). Reductions in air conditioning energy caused by a nearby park. *Energy and Buildings*, *29*(1), 83–92.

Cao, X., Onishi, A., Chen, J., & Imura, H. (2010). Quantifying the cool island intensity of urban parks using ASTER and IKONOS data. *Landscape and Urban Planning*, *96*(4), 224–231.

Chang, C. R., Li, M. H., & Chang, S. D. (2007). A preliminary study on the local cool-island intensity of Taipei city parks. *Landscape and Urban Planning*, *80*(4), 386–395.

Cheng, X., Wei, B., Chen, G., Li, J., & Song, C. (2014). Influence of park size and its surrounding urban landscape patterns on the park cooling effect. *Journal of Urban Planning and Development*, *141*(3), A4014002.

Chow, W. T., Pope, R. L., Martin, C. A., & Brazel, A. J. (2011). Observing and modeling the nocturnal park cool island of an arid city: Horizontal and vertical impacts. *Theoretical and Applied Climatology*, *103*(1-2), 197–211.

Church, R. L., & Murray, A. T. (2009). *Business site selection, location analysis and GIS*. New York: Wileyhttp://dx.doi.org/10.1002/9780470432761.
Church, R., & ReVelle, C. (1974). The maximal covering location problem. *Papers in Regional Science*, *32*(1), 101–118.
City of Phoenix (2010). *Tree and Shade Master Plan*. https://www.phoenix.gov/parkssite/Documents/071957.pdf.
Eliasson, I., & Upmanis, H. (2000). Nocturnal airflow from urban parks-implications for city ventilation. *Theoretical and Applied Climatology*, *66*(1–2), 95–107.
Erell, E., Pearlmutter, D., & Williamson, T. (2012). *Urban microclimate: Designing the spaces between buildings*. Routledgehttp://dx.doi.org/10.4324/9781849775397.
Fan, H., & Sailor, D. J. (2005). Modeling the impacts of anthropogenic heating on the urban climate of Philadelphia: A comparison of implementations in two PBL schemes. *Atmospheric Environment*, *39*(1), 73–84.
Fernández, F. J., Alvarez-Vázquez, L. J., García-Chan, N., Martínez, A., & Vázquez-Méndez, M. E. (2015). Optimal location of green zones in metropolitan areas to control the urban heat island. *Journal of Computational and Applied Mathematics*, *289*, 412–425.
Fung, W. Y., Lam, K. S., Hung, W. T., Pang, S. W., & Lee, Y. L. (2006). Impact of urban temperature on energy consumption of Hong Kong. *Energy*, *31*(14), 2623–2637.
Fung, W. Y., Lam, K. S., Nichol, J., & Wong, M. S. (2009). Derivation of nighttime urban air temperatures using a satellite thermal image. *Journal of Applied Meteorology and Climatology*, *48*(4), 863–872.
Gillespie, A. R., Rokugawa, S., Hook, S. J., Matsunaga, T., & Kahle, A. B. (1999). *Temperature/emissivity separation algorithm theoretical basis document. version 2.4*. Greenbelt, MD: NASA/GSFC. http://eospso.nasa.gov/sites/default/files/atbd/atbd-ast-05-08.pdf.
Gober, P., Brazel, A., Quay, R., Myint, S., Grossman-Clarke, S., Miller, A., et al. (2009). Using watered landscapes to manipulate urban heat island effects: How much water will it take to cool Phoenix? *Journal of the American Planning Association*, *76*(1), 109–121.
Grimm, N. B., Faeth, S. H., Golubiewski, N. E., Redman, C. L., Wu, J., Bai, X., et al. (2008). Global change and the ecology of cities. *Science*, *319*(5864), 756–760.
Grimmond, C. S. B., & Oke, T. R. (2002). Turbulent heat fluxes in urban areas: Observations and a local-scale urban meteorological parameterization scheme (LUMPS). *Journal of Applied Meteorology*, *41*(7), 792–810.
Harlan, S. L., Brazel, A. J., Prashad, L., Stefanov, W. L., & Larsen, L. (2006). Neighborhood microclimates and vulnerability to heat stress. *Social Science & Medicine*, *63*(11), 2847–2863.
Hartz, D. A., Prashad, L., Hedquist, B. C., Golden, J., & Brazel, A. J. (2006). Linking satellite images and hand-held infrared thermography to observed neighborhood climate conditions. *Remote Sensing of Environment*, *104*(2), 190–200.
Hondula, D. M., Davis, R. E., Leisten, M. J., Saha, M. V., Veazey, L. M., & Wegner, C. R. (2012). Fine-scale spatial variability of heat-related mortality in Philadelphia County, USA, from 1983–2008: A case-series analysis. *Environmental Health*, *11*(1), 1.
Hondula, D. M., Vanos, J. K., & Gosling, S. N. (2014). The SSC: A decade of climate–health research and future directions. *International Journal of Biometeorology*, *58*(2), 109–120.
Huang, G., Zhou, W., & Cadenasso, M. L. (2011). Is everyone hot in the city? Spatial pattern of land surface temperatures, land cover and neighborhood socioeconomic characteristics in Baltimore, MD. *Journal of Environmental Management*, *92*(7), 1753–1759.
JPL (2001). *ASTER higher-level product user guide, advanced spaceborne thermal emission and reflection radiometer*. Jet Propulsion Laboratory, California Institute of Technologyhttp://asterweb.jpl.nasa.gov/content/03_data/04_Documents/ASTERHigherLevelUserGuideVe.
Jenerette, G. D., Harlan, S. L., Stefanov, W. L., & Martin, C. A. (2011). Ecosystem services and urban heat riskscape moderation: Water, green spaces, and social inequality in Phoenix, USA. *Ecological Applications*, *21*(7), 2637–2651.
Klok, L., Zwart, S., Verhagen, H., & Mauri, E. (2012). The surface heat island of Rotterdam and its relationship with urban surface characteristics. *Resources, Conservation and Recycling*, *64*, 23–29.
Li, X., Zhou, W., & Ouyang, Z. (2013). Relationship between land surface temperature and spatial pattern of greenspace: What are the effects of spatial resolution? *Landscape and Urban Planning*, *114*, 1–8.
Li, X., Myint, S. W., Zhang, Y., Galletti, C., Zhang, X., & Turner, B. L. (2014). Object-based land-cover classification for metropolitan Phoenix, Arizona, using aerial photography. *International Journal of Applied Earth Observation and Geoinformation*, *33*, 321–330.
Li, X., Li, W., Middel, A., Harlan, S. L., & Brazel, A. J. (2016). Remote sensing of the surface urban heat island and land architecture in Phoenix, Arizona: Combined effects of land composition and configuration and cadastral-demographic-economic factors. *Remote Sensing of Environment*, *174*, 233–243.
Lin, W., Yu, T., Chang, X., Wu, W., & Zhang, Y. (2015). Calculating cooling extents of green parks using remote sensing: Method and test. *Landscape and Urban Planning*, *134*, 66–75.
McGarigal, K., Marks, B.J., FRAGSTATS: spatial pattern analysis program for quantifying landscape structure, 1995.
Meier, A., & Taha, H. (2000). Mitigation of urban heat islands: Meteorology, energy, and air quality impact. *Journal of Architecture, Planning and Environmental Engineering*, *529*, 69–76.
Middel, A., Chhetri, N., & Quay, R. (2015). Urban forestry and cool roofs: Assessment of heat mitigation strategies in Phoenix residential neighborhoods. *Urban Forestry & Urban Greening*, *14*(1), 178–186.
Murray, A. T., Tong, D., & Kim, K. (2010). Enhancing classic coverage location models. *International Regional Science Review*, *33*(2), 115–133.
Myint, S. W., Wentz, E. A., Brazel, A. J., & Quattrochi, D. A. (2013). The impact of distinct anthropogenic and vegetation features on urban warming. *Landscape Ecology*, *28*(5), 959–978.
Myint, S. W., Zheng, B., Talen, E., Fan, C., Kaplan, S., Middel, A., et al. (2015). Does the spatial arrangement of urban landscape matter? Examples of urban warming and cooling in Phoenix and Las Vegas. *Ecosystem Health and Sustainability*, *1*(4), 1–15.
Neema, M. N., & Ohgai, A. (2013). Multitype green-space modeling for urban planning using GA and GIS. *Environment and Planning B: Planning and Design*, *40*(3), 447–473.
Ng, E., Chen, L., Wang, Y., & Yuan, C. (2012). A study on the cooling effects of greening in a high-density city: an experience from Hong Kong. *Building and Environment*, *47*, 256–271.
Nichol, J. E., Fung, W. Y., Lam, K. S., & Wong, M. S. (2009). Urban heat island diagnosis using ASTER satellite images and 'in situ'air temperature. *Atmospheric Research*, *94*(2), 276–284.
Ren, Z., He, X., Zheng, H., Zhang, D., Yu, X., Shen, G., et al. (2013). Estimation of the relationship between urban park characteristics and park cool island intensity by remote sensing data and field measurement. *Forests*, *4*(4), 868–886.
Ruddell, D. M., Harlan, S. L., Grossman-Clarke, S., & Buyantuyev, A. (2010). *Risk and exposure to extreme heat in microclimates of Phoenix, AZ. Geospatial techniques in urban hazard and disaster analysis*, . Netherlands: Springer, 179–202. http://dx.doi.org/10.1007/978-90-481-2238-7_9.
Ruddell, D., Hoffman, D., Ahmad, O., & Brazel, A. (2013). Historical threshold temperatures for Phoenix (urban) and Gila Bend (desert), central Arizona, USA. *Climate Research*, *55*(3), 201–215.
Sailor, D. J. (2001). Relating residential and commercial sector electricity loads to climate-evaluating state level sensitivities and vulnerabilities. *Energy*, *26*(7), 645–657.
Shashua-Bar, L., Pearlmutter, D., & Erell, E. (2009). The cooling efficiency of urban landscape strategies in a hot dry climate. *Landscape and Urban Planning*, *92*(3), 179–186.
Spronken-Smith, R. A., & Oke, T. R. (1998). The thermal regime of urban parks in two cities with different summer climates. *International Journal of Remote Sensing*, *19*(11), 2085–2104.
Spronken-Smith, R. A., & Oke, T. R. (1999). Scale modelling of nocturnal cooling in urban parks. *Boundary-Layer Meteorology*, *93*(2), 287–312.
Spronken-Smith, R. A., Oke, T. R., & Lowry, W. P. (2000). Advection and the surface energy balance across an irrigated urban park. *International Journal of Climatology*, *20*(9), 1033–1047.
Stoll, M. J., & Brazel, A. J. (1992). Surface-air temperature relationships in the urban environment of Phoenix, Arizona. *Physical Geography*, *13*(2), 160–179. http://dx.doi.org/10.1080/02723646.1992.10642451.
Turner, B. L., Janetos, A. C., Verburg, P. H., & Murray, A. T. (2013). Land system architecture: Using land systems to adapt and mitigate global environmental change. *Global Environmental Change*, *23*(2), 395–397. http://dx.doi.org/10.1016/j.gloenvcha.2012.12.009.
Upmanis, H., Eliasson, I., & Lindqvist, S. (1998). The influence of green areas on nocturnal temperatures in a high latitude city (Göteborg, Sweden). *International Journal of Climatology*, *18*(6), 681–700.
Voogt, J. A., & Oke, T. R. (2003). Thermal remote sensing of urban climates. *Remote Sensing of Environment*, *86*(3), 370–384.
Weng, Q. (2009). Thermal infrared remote sensing for urban climate and environmental studies: Methods, applications, and trends. *ISPRS Journal of Photogrammetry and Remote Sensing*, *64*(4), 335–344.
Wentz, E. A., Rode, S., Li, X., Tellman, E. M., & Turner, B. L. (2016). Impact of Homeowner Association (HOA) landscaping guidelines on residential water use. *Water Resources Research*, *52*, 3373–3386. http://dx.doi.org/10.1002/2015WR018238.
Zhang, W., & Huang, B. (2014). Land use optimization for a rapidly urbanizing city with regard to local climate change: Shenzhen as a case study. *Journal of Urban Planning and Development*, *141*(1), 05014007.
Zhou, W., Huang, G., & Cadenasso, M. L. (2011). Does spatial configuration matter? Understanding the effects of land cover pattern on land surface temperature in urban landscapes. *Landscape and Urban Planning*, *102*(1), 54–63.